Iranian Journal of Chemical Engineering
Vol. 16, No. 3 (Summer 2019), IAChE

Computational Fluid Dynamics Study of and GA Modeling Approach to the Bend Angle Effect on Thermal-Hydraulic Characteristics in Zigzag Channels

S. Salimi, R. Beigzadeh [*]

Department of Chemical Engineering, Faculty of Engineering, University of Kurdistan, Sanandaj, Iran

ARTICLE INFO

Article history:
Received: 2019-09-14
Accepted: 2019-12-26

Keywords:
Zigzag Serpentine Channel,
Bend Angle,
Turbulent Flow,
Computational Fluid Dynamics (CFD),
Genetic Algorithm

ABSTRACT

In this study, the thermal-hydraulic performance of the zigzag channels with a circular cross-section was analyzed by Computational Fluid Dynamics (CFD). The standard K-ε turbulent scalable wall functions were used for modeling. The wall temperature was assumed constant as 353 K and water was used as the working fluid. The zigzag serpentine channels with bend angles of 5-45° were studied for turbulent flow from 4000 to 40,000 Reynolds number (Re). The thermal performance of the zigzag 45° channel was better than that of the other channels, and also it had the highest friction factor (f). The bends caused secondary flow and, as the bend angle increased, the secondary flow increased. This Phenomenon had a positive effect on thermal performance and a negative effect on hydraulic performance by increasing the friction factor. The obtained CFD data were used to develop correlations for predicting the Nu and f as the functions of Re and bend angles. The correlation constants were optimized by the genetic algorithm method, which led to the mean relative errors of 3.32 % and 6.94 % for Nu and f estimation, respectively.

1. Introduction

In recent years, extensive studies have been done to increase the efficiency of heat exchangers, which indicates the importance of preventing excessive energy dissipation and increasing the efficiency of heat exchangers. However, very few studies have been performed on the thermal-hydraulic performance (THP) of zigzag serpentine channels (especially in turbulent flows). For this reason, researching these types of channels will be useful and practical.

Heat exchangers are the most important tools in process operations [1]. Serpentine channels are applied and used in microchannel reactors and heat exchangers. These types of channels exhibit better mixing, higher mass, and heat transfer coefficients than those of straight and simple channels [2]. Potential heat transfer enhancement in heat exchanger devices has recently increased great popularity because of the importance of these devices in numerous engineering applications. There are various methods for improving heat transfer in heat exchangers. One way to increase heat transfer

[*]Corresponding author: r.beigzadeh@uok.ac.ir

performance and efficiency of the heat exchanger is to use optimum characteristics of channel geometry that produce minimum pressure drop [3]. The pipe bends are the most important parts of any pipe line system as they provide flexibility in routing. Investigations and studies of the flow through bends are of great matter in understanding and amending their performance and minimizing the losses [4-6]. Water flow through channel bends is found in many engineering applications. Some researchers have studied turbulent flows in channel bends by means of theoretical, experimental, and numerical methods [7-10]. Curved channels are characterized by compact structures and good hydro-thermal performance; therefore, the transport phenomena (i.e. momentum, heat, and mass) happening in these geometries are more wrapped than those in straight channels. As the fluid passes through the helical, serpentine, or spiral channels, the attendance of curvatures in the fluid path leads to centrifugal forces, thereby rotational flows are induced that have a meaningful ability to increase the rate of transport phenomena. Actually, the performance of curved channels depends on the manner of generated rotational flows [11]. Ngo et al. [12] extended the experimental correlations of Nu and pressure drop factors of S-shaped and zigzag channel microchannel heat exchangers (MCHEs). A computational fluid dynamics based method was developed to study the flow and heat transfer in periodic zigzag channels with square cross-sections for steady-state laminar flow, and that method covers Reynolds numbers ranging from 50 to 400 [13].

The computational fluid dynamics (CFD) technique is widely employed to model the heat transfer systems. Keshavarz Moraveji and Beheshti [14] investigated the CFD modeling for the heat transfer system including adding nanoparticles such as Al_2O_3, TiO_2, and CuO to pure fluids to improve thermal performance. Beigzadeh [15] applied the CFD to provide data for an adaptive neuro-fuzzy inference system (ANFIS) for modeling the thermal characteristics in flat and discontinuous fins.

The secondary flow in the serpentine channel has a significant effect on the THP, which enhances the mixing of fluid and prevents the expansion of the boundary layer. The secondary flow amends the scope synergy between temperature and velocity gradient, which finally enhances the heat transfer function. The Prandtl number affects thermal performance seriously, especially near the pseudo-critical point [16].

In this study, the effects of bend angle on secondary flow formation and THP of the channels were studied. The THP of zigzag serpentine channels at a 0-45° bend angle for Re 4000 to 40,000 was investigated, and the effect of bend angle and Reynolds number parameters on thermal and hydraulic factors was studied. The boundary conditions in this modeling were different from those in previous studies. The obtained CFD data were employed for developing correlations by genetic algorithm. The developed equations are very reliable due to a wide range of considered factors.

2. Numerical approach

2.1. Physical model and boundary conditions

In this study, the THP of serpentine zigzag and straight channels was investigated. The length of all channels was 2.2 m and their hydraulic diameter was 1 cm. The zigzags consist of channels with a bending angle of 5-

45°. Each piece in the zigzag channels was 10 cm in length, and there were pitch 10 pitches of the bends in all of channels. The structure of Hex-Wedge mesh type was selected for meshing geometries. The velocity inlet was selected at the inlet of straight and zigzag channels, while the pressure outlet boundary condition was selected at the outlet of models. The wall thickness was considered to be negligible, and its temperature was constant in 353 K throughout the channel. The inlet temperature for all channels was 298 K. In geometries, the boundary layer meshing was used to model the turbulent flow behavior and thermal-hydraulic gradients near the walls more precisely.

The bend angle of each channel is reported in Table 1. Fig. 1 illustrates the geometrical properties used in the modeling such as the number of pitches, length of channel, bend angle, hydraulic diameter, section length, and boundary conditions in a general and symbolic manner.

Table 1
The bend angle for each case.

Case number	1	2	3	4	5	6	7	8	9	10
Θ (°)	0	5	10	15	20	25	30	35	40	45

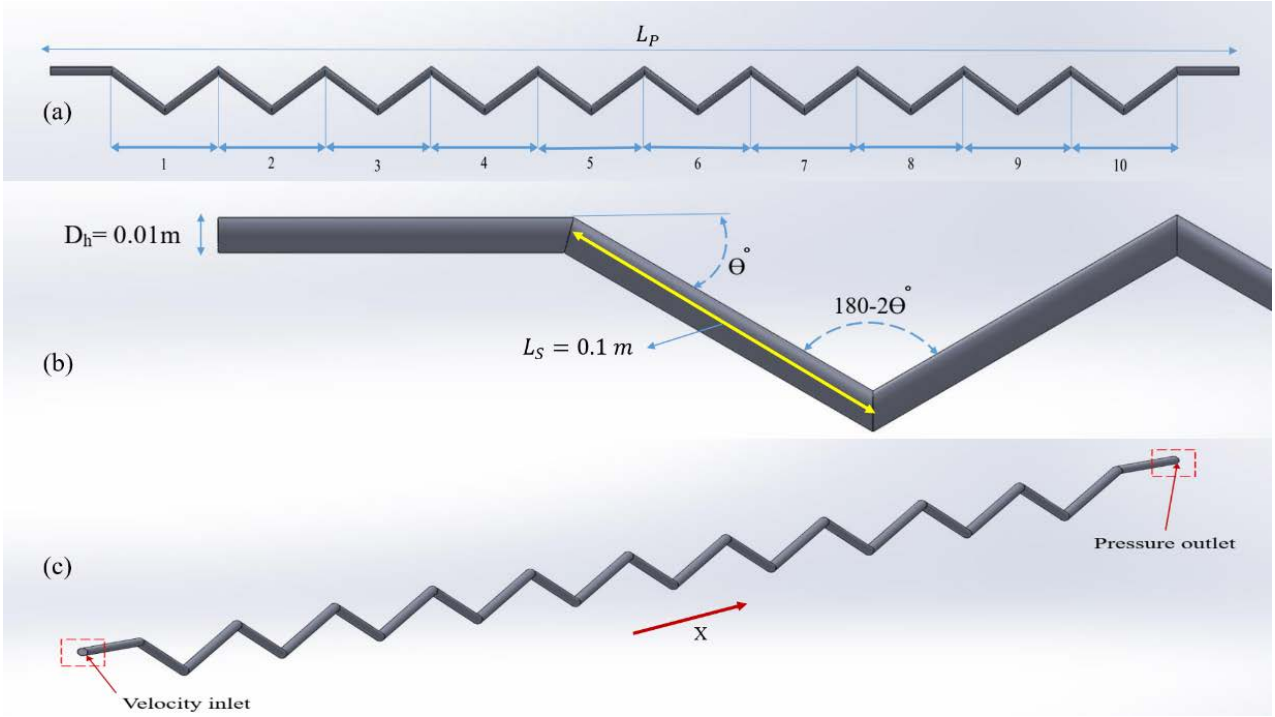

Figure 1. Schematic of (a) number of pitches in zigzag serpentine channels; (b) geometric parameters of zigzag serpentine channels; (c) boundary condition of the model.

2.2. Numerical method and gird independence

The hardware used to perform the modeling processes was characterized by Core i7 7500 HQ, Ram 8G, and Graphic 4G. The numerical solution was performed on the 3D model. Double-precision and pressure-based solvers were selected for this study. The standard K-ε model was chosen, and the scalable wall function was employed to increase the

accuracy of the simulation. Choosing the type of near wall treatment has a direct relation with the value of Y^+ (Dimensionless thickness or distance of the first boundary layer mesh from the wall). For $30 < Y^+ < 300$, the scalable wall function showed the best performance, and the size of the boundary layer mesh was the most important factor in choosing the right model. The SIMPLE scheme was selected to establish pressure-velocity coupling. The momentum and energy using second-order upwind and turbulent kinetic energy and turbulent dissipation rate scheme using first-order upwind were discretized. The residuals were less than 10^{-6} considering the convergence of calculations. The thermo-physical properties of the water were considered based on the average temperature of the fluid bulk at the inlet and outlet of channels. The mesh was performed independently to ensure simulation. The percentage error less than 0.01 for pressure drop was the selected criterion to select the best number of meshes. The obtained pressure drops for different meshes are shown in Fig. 2. According to the figure, about 500,000 cells were chosen for the meshing procedure. In Fig. 3, the meshing type and the computational domain are shown. The boundary layer mesh has been used to improve the accuracy of the computations.

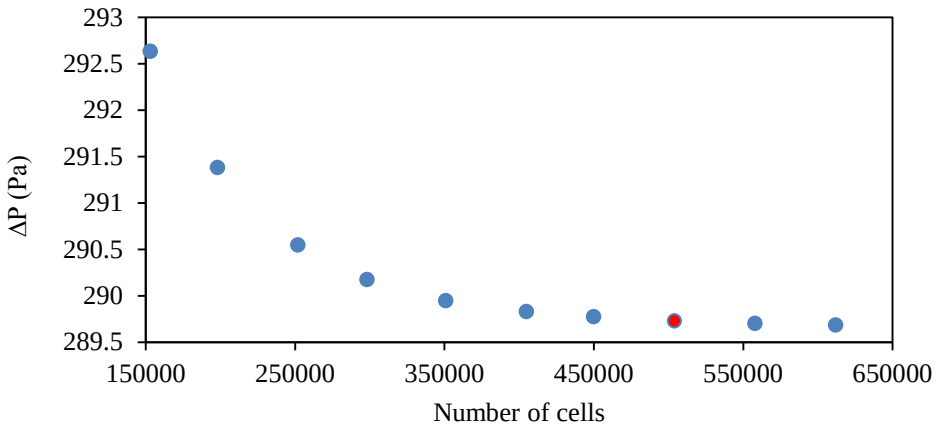

Figure 2. Effect of the cell number on pressure drop results.

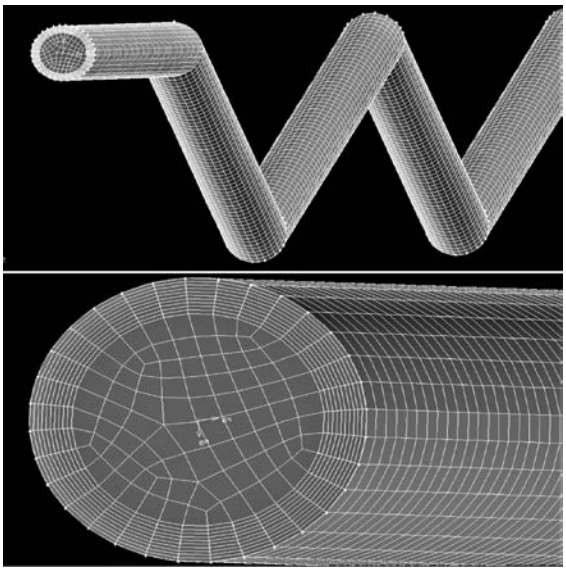

Figure 3. Schematic of the computational domain and meshing type.

The governing equations used to study heat transfer include continuity, momentum, and energy equations as follows:

To calculate the continuity equation, we get:

$$\frac{\partial}{\partial x_i}(\rho u_i) = 0 \qquad (1)$$

in which ρ is the density, and u_i is the velocity vector.

Momentum equation is calculated as follows:

$$\frac{\partial}{\partial x_i}\left(\rho u_i u_j\right) = -\frac{\partial P}{\partial x_i} + \frac{\partial}{\partial x_j}\left[(\mu + \mu_t)\frac{\partial u_i}{\partial x_j}\right] \qquad (2)$$

where P is the pressure, and μ_t and μ are

turbulent and molecular viscosities.

Energy equation is calculated by:

$$\frac{\partial}{\partial x_i}(u_i(\rho E + p)) = \frac{\partial}{\partial x_i}(k_{eff}\frac{\partial T}{\partial x_i} + u_i\tau_{ij}) \quad (3)$$

where k_{eff} is the effective conductivity; $k_{eff} = k + k_t$, and k_t is the turbulent thermal conductivity.

The logarithmic mean temperature difference between the balcony and the wall is calculated through the following formula:

$$\Delta T_{LMTD} = \frac{(t_w - t_i) - (t_w - t_o)}{\ln(\frac{t_w - t_i}{t_w - t_o})} \quad (4)$$

To calculate the heat transfer rate, we use:

$$\dot{Q} = \dot{m}C_P(t_o - t_i) \quad (5)$$

The convection heat transfer coefficient is obtained based on the logarithmic mean temperature difference and the convection heat transfer rate:

$$h = \frac{\dot{Q}}{A\Delta T_{LMTD}} \quad (6)$$

To calculate the friction factor, Reynolds number, and Nusselt number, we have:

$$f = \frac{2\Delta P D_h}{\rho u^2 L_P} \quad (7)$$

$$Re = \frac{\rho u D_h}{\mu} \quad (8)$$

$$Nu = \frac{hD_h}{k} \quad (9)$$

The transfer equations for the Standard $k - \varepsilon$ Model are defined as follows:

For turbulent kinetic energy (k):

$$\frac{\partial}{\partial t}(\rho k) + \frac{\partial}{\partial x_i}(\rho k u_i) = \frac{\partial}{\partial x_j}\left[\left(\mu + \frac{\mu_t}{\sigma_k}\right)\frac{\partial k}{\partial x_j}\right] + P_k + \rho\varepsilon \quad (10)$$

For dissipation energy (ε):

$$\frac{\partial}{\partial t}(\rho\varepsilon) + \frac{\partial}{\partial x_i}(\rho\varepsilon u_i) = \frac{\partial}{\partial x_j}\left[\left(\mu + \frac{\mu_t}{\sigma_\varepsilon}\right)\frac{\partial \varepsilon}{\partial x_j}\right] + C_{1\varepsilon}\frac{\varepsilon}{k}(P_k) - C_{2\varepsilon}\rho\frac{\varepsilon^2}{k} \quad (11)$$

To measure the thermal-hydraulic performance (THP) of the channels [17], the following is used:

$$THP = \frac{Nu/Nu_S}{(f/f_S)^{1/3}} \quad (12)$$

The model validation was limited due to the scarcity of studies related to turbulent flow in zigzag channels. The following empirical formula was used to compare the modeled and empirical Nu's for the straight channel. The Taler and Taler Formula [18] is used as follows:

$$Nu = 0.00881Re^{0.8991}Pr^{0.3911} \quad (13)$$

$$3 \times 10^3 \leq Re \leq 10^6 \;\; ; \;\; 3 < Pr \leq 1000$$

They presented an empirical formula for turbulent flows in circular cross-section straight channels. By using empirical data, three power-type correlations for Nu were obtained according to the Re and Pr ranges. The simulations were initially performed for the straight channels in the Re range of 4000 to 40000. The obtained Nu from Eq. (13) and simulations were compared for the validation of the CFD results. Since the simulation error was low and acceptable, then simulation was performed for zigzag channels. A comparison between experimental and simulated results is reported in Table 2. The difference of Nu between the modeling and experimental formulas was within an acceptable range.

Based on the past experiences found in the literature [19, 20], the K-Omega model was more reliable for the low Re (near transient flow) and the K-Ɛ model was well suited for the higher Re. In Table 2, as known, as Re increased, the error rate between the experimental and simulated results decreased. The modeling with other models needed

much time due to the hardware limitations. On the other hand, the investigated models did not have a complex geometry, and there was no significant difference in the final answers. The best model with acceptable accuracy and processing time was K-Ɛ model, and it supported the boundary layer mesh and did not require the resizing of the boundary layer mesh in the larger range of Re.

Table 2
Relative error of simulation and experiment results for Nu number.

Re	Nu (simulated)	Nu (experimental)	Error (%)
4000	29.01	26.28	9.42
8000	54.03	49.21	8.94
12000	77.52	71.13	8.24
16000	99.87	92.44	7.44
20000	121.20	113.27	6.54
24000	141.78	133.79	5.64
28000	161.76	154.08	4.75
32000	181.22	174.18	3.88
36000	200.13	194.00	3.06
40000	218.94	213.69	2.40

3. Results and discussion

The THP for the straight and zigzag serpentine channels with the bending angles of 5-45° in the Reynolds number range of 4000 to 40,000 was investigated. Totally, 100 different layouts of bending angle and Reynolds number variables were investigated.

In the investigated heat exchangers, increasing the heat transfer efficiency leads to the increasing the pressure drop, which is an undesirable factor. For this reason, it has always been important to choose an optimal geometry based on the goals set. All results showed a very slight difference in the outlets of the straight and zigzag 5° channels, and their thermal-hydraulic performance was almost the same; moreover, practically, the straight channel was more economical and easier to use than the zigzag 5° channel. At higher bend angles, the performance difference of the pipes increased.

The velocity contours for Steps 4 to 6 at angles 0-45° for Reynolds number 20000 are shown in Fig. 4. At the corner of the bends and the tangential area (after each bending), the area of dead state and inactivity was formed and expanded. The fluid velocity increased at the moment it hit the front surface and passed the bend. The increasing bend angle led to developing the secondary flow after the fluid passed through the bends. The highest value of secondary flow was observed in the zigzag channel of 45° angle. The secondary flow intensification leads to an increase in the pressure drop and convection heat transfer in secondary flow areas than those in other regions.

The temperature changes along the channels are shown in Fig. 5. As the bending angle increased at a constant Re, an increase in temperature gradient was observed due to the disruption of the thermal boundary layer. After crossing the bends, the opportunity for heat exchange increased due to the disruption

of the thermal boundary layer. At high bending angles, the rotational motion of the fluid and the pressure drop increased and the temperature gradient increased to a greater degree. These effects result from the creation and reinforcement of secondary flow in bends and corners. The highest displacement heat transfer rate was observed at the sites where this phenomenon occurred. According to the comparison of Figs. 4 and 5, the coordinates of secondary flow and their temperature are visible.

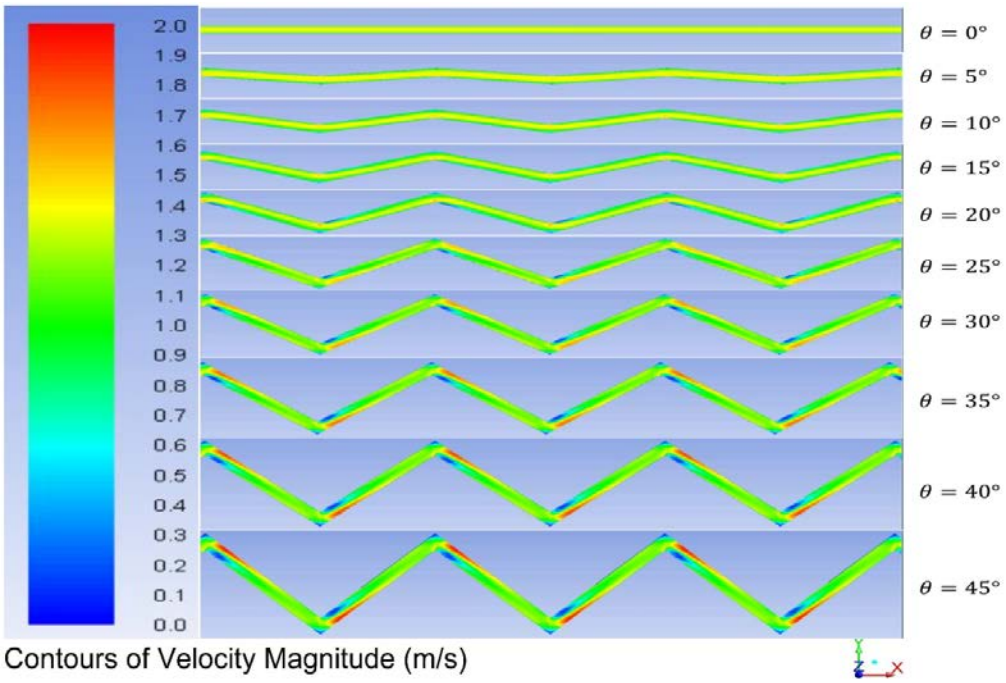

Figure 4. Velocity contours of pitches = 4-6 at bend angles of 0-45° at Re = 20000.

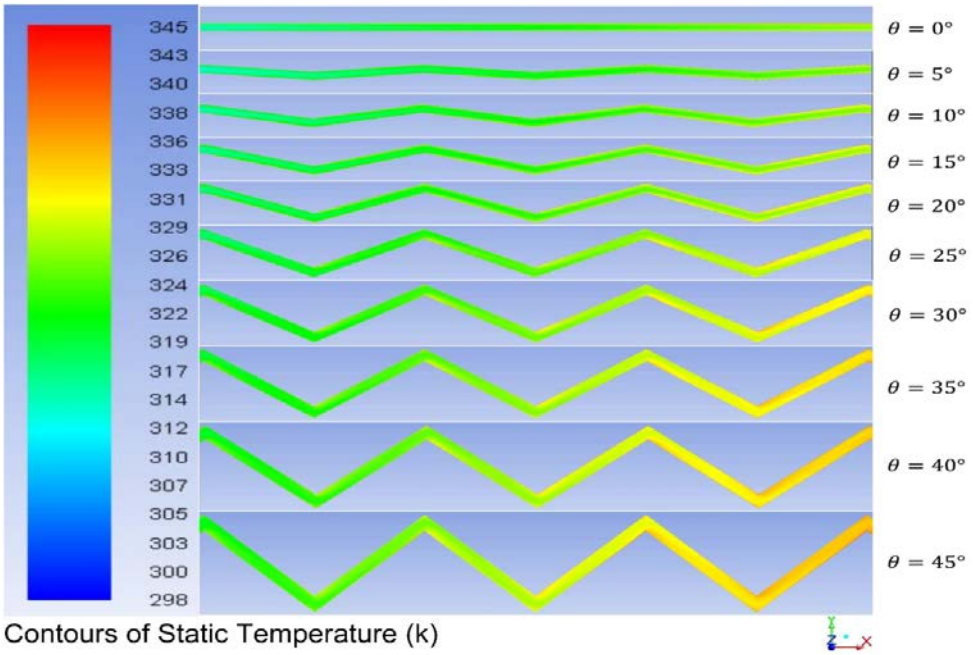

Figure 5. Temperature contours of pitches = 4-6 at bend angles of 0-45° in Re = 20000.

Fig. 6 shows the turbulence intensity contours at bending angles of 0-45°. With increasing bending angles, the intensity of flow turbulence (especially after each bend) increased in the channel. An increase in turbulence intensity after each bend was due to two factors: increasing secondary flow after each bend and increasing fluid velocity in the adjacent areas. This phenomenon has led to a drastic change in the pattern of fluid flow.

As can be seen in Fig. 7, the highest outlet fluid temperature belongs to the channel with a bend angle of 45°. The increasing bend angle leads to a decrease in the thickness of the thermal boundary layer and an increase in the flow mixing. The increasing trend of the difference between the outlet fluid temperature for the straight and zigzag 45° channels was observed, which increased from 5.25 K from Re=4000 to 4.3 K at Re=40000. This clearly demonstrates the effect of bend angle at high Re on increasing the outlet fluid temperature and thermal performance in the channels.

As shown in Fig. 7, the outlet temperature decreased by increasing Reynolds number in all channels. Increasing the Reynolds number shortened the fluid retention time in the tube, which again shortened the contact time between the wall and fluid. Fig. 8 shows the variation of the heat transfer coefficient with Re for all investigated cases. The convection heat transfer increased by increasing Re and bend angle due to the decreasing thermal boundary layer. The difference of the heat transfer coefficient between straight and zigzag 45° channels widened by increasing Re. The difference increased from 594.46 $\frac{W}{m^2.K}$ at Re=4000 to 4965.5 $\frac{W}{m^2.K}$ at Re=40000. By increasing the bend angle, the thermal boundary layer was disrupted, and the rate of heat transfer from the channel surface to the fluid increased.

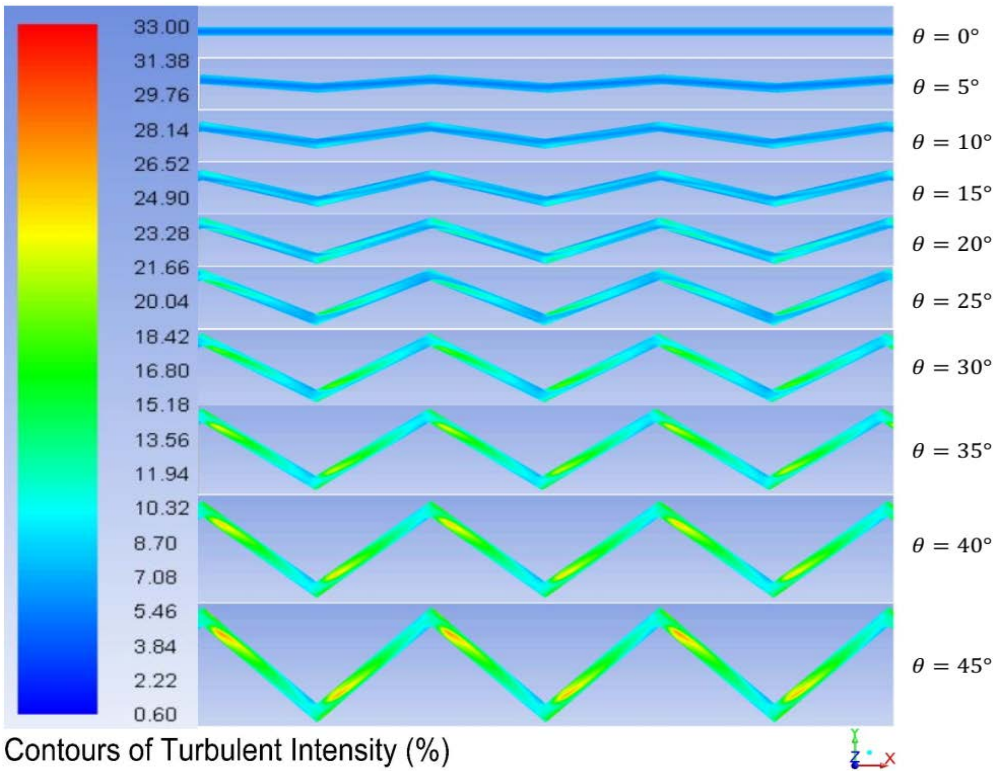

Figure 6. Turbulent intensity contours of pitches = 4-6 at bend angles of 0-45° at Re = 20000.

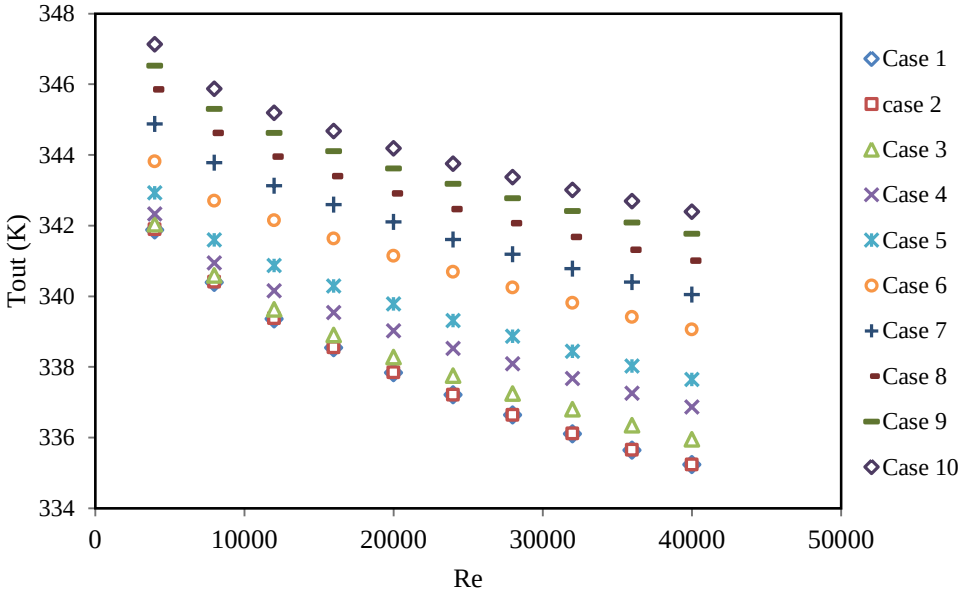

Figure 7. Outlet temperature of the zigzag channels at different Re.

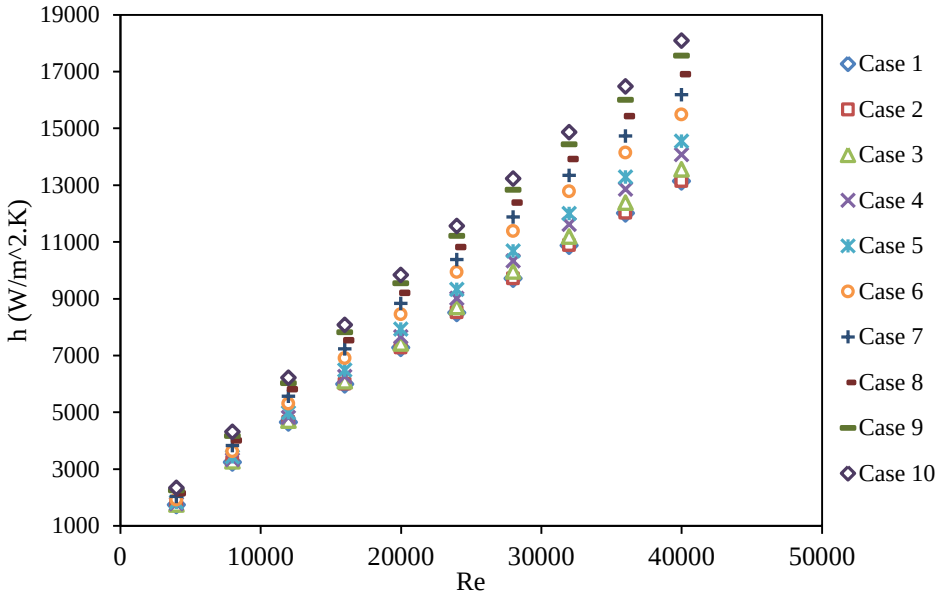

Figure 8. Heat transfer coefficient of the zigzag channels at different Re.

By increasing the Reynolds number shown in Fig. 9, the pressure drop increased, thereby the power and costs of fluid pumping in the channels increased. At high Re, the slope of the fluid pumping cost for the high bend angle channels increased greatly, which is a weakness for the hydraulic performance for the high bend angle zigzag channels. By increasing the bend angle and Re, the pressure drop increased extremely. Increasing the bend angle strengthened the secondary flows in the bend regions and increased the pressure drop.

The wall shear stress, shown in Fig. 10, intensified with an increase in the bending angle due to an increase in flow turbulence in the bending area wall and an increase in the velocity gradient. The rate of the increase of the velocity gradient was higher than that of

the decrease of dynamic viscosity. As Reynolds increased, the velocity gradient on the channel wall surface increased, too. As a result, the shear force imposed on the surface increased. In the bend regions, because of sudden changes in the velocity gradient in terms of magnitude and vector and the phenomenon of secondary currents, higher wall shear stress occurred.

The variation of the thermal-hydraulic performance (THP) of the investigated zigzag channels is illustrated in Fig. 11. As the bending angle increased, the thermal-hydraulic performance of the channels decreased. According to Eq. 12, the rate of the increasing Nu was lower than that of the increasing friction factor. At bend angles above 30 °, an increase in Re had a more negative effect on efficiency.

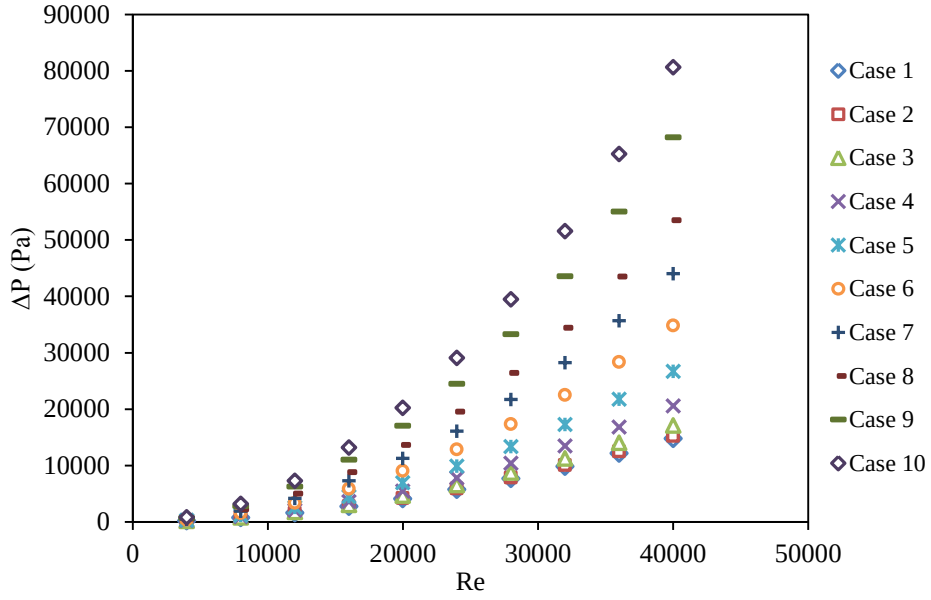

Figure 9. Pressure drop of the zigzag channels at different Re.

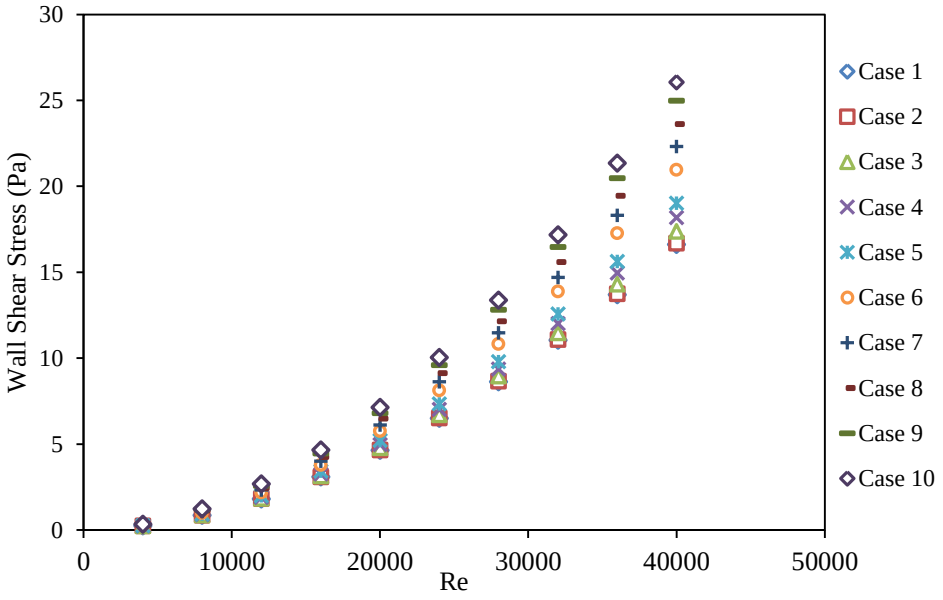

Figure 10. Wall shear stress of the zigzag channels at different Re.

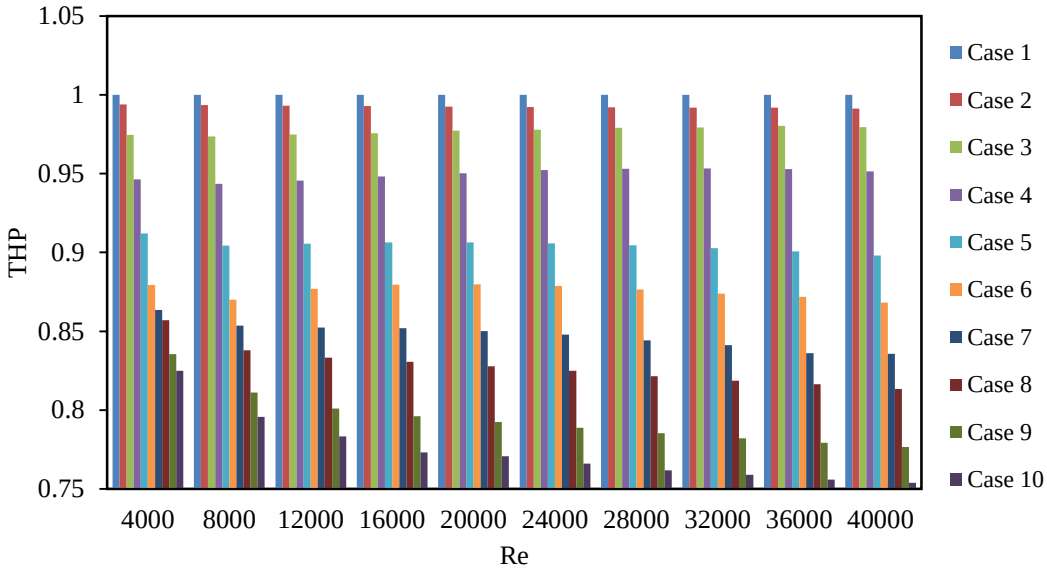

Figure 11. The thermal-hydraulic performance (THP) of the zigzag channels at different Re.

3.1. Developing correlations by genetic algorithm

The genetic algorithm (GA) searching method was used to propose prediction correlations for the investigated zigzag channels. The output CFD data were used to develop novel correlations for predicting the Nusselt number (Nu) and friction factor (f). Different forms of the equations were investigated, and the equations with higher accuracy were selected. Finally, the following equations were considered:

$$\mathrm{Nu} = \mathrm{C_1}\,\mathrm{Re}^{\mathrm{C_2}}\mathrm{Pr}^{\mathrm{C_3}}\left(1+\left(\theta/\pi\right)^{\mathrm{C_4}}\right) \tag{14}$$

$$\mathrm{f} = \mathrm{C_1'}\,\mathrm{Re}^{\mathrm{C_2'}}\left(1+\theta/\pi\right)^{\mathrm{C_3'}} \tag{15}$$

where C_i and C_i' are the constants. The fitness functions from the target and estimated data are defined through average squared deviation (ASD) as follows:

$$\mathrm{ASD_{Nu}}(\mathrm{C_1},\mathrm{C_2},\mathrm{C_3},\mathrm{C_4}) = \frac{1}{\mathrm{N}}\sum_{\mathrm{i=1}}^{\mathrm{N}}(\mathrm{Nu_i^{target}} - \mathrm{Nu_i^{estimated}}) \tag{16}$$

$$\mathrm{ASD_f}(\mathrm{C_1'},\mathrm{C_2'},\mathrm{C_3'}) = \frac{1}{\mathrm{N}}\sum_{\mathrm{i=1}}^{\mathrm{N}}(\mathrm{f_i^{target}} - \mathrm{f_i^{estimated}}) \tag{17}$$

where N is the number of data points. The fitness functions were minimized by GA. The primary population size of 200, the crossover fraction of 0.8, and elite offspring of 2 were considered. Details related to the genetic algorithm approach used for the optimization process were described by Rahimi et al. [21]. The GA was used to develop the correlations due to the superiority of the method to traditional methods such as the least square technique. The correlation constants are determined as follows:

$$\mathrm{Nu} = 0.016\,\mathrm{Re}^{0.897}\mathrm{Pr}^{0.005}\left(1+\left(\theta/\pi\right)^{0.816}\right) \tag{18}$$

$$\mathrm{f} = 0.047\,\mathrm{Re}^{-0.091}\left(1+\theta/\pi\right)^{8.966} \tag{19}$$

The comparison between the target and estimated data led to the mean relative errors of 3.32 % and 6.94 % for Nu and f, respectively.

4. Conclusions

In this study, the flow and heat transfer parameters of water liquid in zigzag channels were investigated by using CFD in different operating conditions. The CFD model was used to quantify the effect of different hydraulic and geometrical parameters of zigzag channels (bend angle and Reynolds number) on heat transfer and pressure drop. The results showed that increasing the bend angle created and improved the secondary flow at the corners and after each bend. The secondary flow was strengthened by increasing Re and contributed to the increased convection heat transfer rate. In all channels, most of the effects and results of the Re and bend angle variations were observed in the areas after each bend. The pressure drop, turbulent intensity, and the heat transfer after each bend increased with a higher slope. By increasing the bend angle at constant Re, the outlet fluid temperature and convection heat transfer coefficient increased (positive effects on thermal performance). Moreover, the pressure drop and wall shear stress increased (negative effects on hydraulic performance). At Re 4000, the pressure drop and heat transfer coefficient in the zigzag channel of 45° angle compared to the straight channel were associated with the increase rates of 294 % and 34 %, respectively. However, the thermal-hydraulic performance (THP) of the zigzag channel decreased by 18%. On the other hand, compared to the straight channel, at Re 40000, pressure drop and heat transfer coefficient in the 45° zigzag channel were associated with the increase of 444 % and 38 %, respectively. However, THP of the zigzag channel decreased by 25% compared to the straight channel.

In addition, two predictive correlations were developed for the investigated zigzag channels. The suitable correlation constants were obtained by the GA searching approach. The comparison results between the target and predicted values indicate the high accuracy of the modeling.

Nomenclature

T	temperature [K].
s	straight channel.
P	pressure [Pa].
L_P	length of path flow [m].
L_S	length of sections [m].
u	velocity [m/s].
Re	Reynolds number.
Nu	Nusselt number.
h	convection heat transfer coefficient [$W/m^2.K$].
$\dot{Q}$	convection heat transfer rate [$W/m^2.s$].
f	friction factor.
τ	wall shear stress [Pa].
ΔP	pressure drop [Pa].
Pr	Prandtl number.
C_P	specific heat [J/Kg.K].
k	thermal conductivity [W/m.K].
D_h	hydraulic diameter [m].
THP	thermal-hydraulic performance [%].
P_k	production of kinetic energy [$kg/m.s^3$].

Greek symbols

μ	viscosity [Pa.s].
ρ	density [kg/m^3].
ε	turbulent dissipation rate [m^2/s^3].

References

[1] Beigzadeh, R., Parvareh, A. and Rahimi, M., "Experimental and CFD study of the tube configuration effect on the shell-side thermal performance in a shell and helically coiled tube heat exchanger", *Iran J. Chem. Eng.*, **12** (2), 13 (2015).

[2] Karale, C. M., Bhagwat, S. S. and Ranade, V. V., "Flow and heat transfer in serpentine channels", *AIChE J.*, **59** (5), 1814 (2013).

[3] Ozbolat, V., Tokgoz, N. and Sahin, B., "Flow characteristics and heat transfer

enhancement in 2D corrugated channels", *Int. J. Mech. Sci. Eng.*, **7** (10), 796 (2013).

[4] Arvanitis, K. D., Bouris, D. and Papanicolaou, E., "Laminar flow and heat transfer in U-bends: The effect of secondary flows in ducts with partial and full curvature", Int. J Therm. Sci., 130, 70 (2018).

[5] Takamura, H., Ebara, S., Hashizume, H., Aizawa, K. and Yamano, H., "Flow visualization and frequency characteristics of velocity fluctuations of complex turbulent flow in a short elbow piping under high Reynolds number condition", *J. Fluids Eng.*, **134** (10), 101201 (2012)

[6] Kim, J., Yadav, M. and Kim, S., "Characteristics of secondary flow induced by 90-degree elbow in turbulent pipe flow", *Eng. Appl. Comp. Fluid Mech.*, **8** (2), 229 (2014).

[7] Sheikholeslami, M., Gerdroodbary, M. B., Mousavi, S. V., Ganji, D. D. and Moradi, R. "Heat transfer enhancement of ferrofluid inside an 90 elbow channel by non-uniform magnetic field", *J. Magn. Magn. Mater*, **460**, 302 (2018).

[8] Naphon, P. and Wongwises, S., "A review of flow and heat transfer characteristics in curved tubes", *Renew. Sustain. Energy Rev.*, **10** (5), 463 (2006).

[9] Wang, J., Wang, S., Zhang, T. and Battaglia, F., "Numerical and analytical investigation of ice slurry isothermal flow through horizontal bends", *Int. J. Refrig.*, **92**, 37 (2018).

[10] Kalpakli, A. and Örlü, R., "Turbulent pipe flow downstream a 90 pipe bend with and without superimposed swirl", *Int. J. Heat Fluid Flow*, **41**, 103 (2013).

[11] Khoshvaght-Aliabadi, M., Khaligh, S. F. and Tavassoli, Z., "An investigation of heat transfer in heat exchange devices with spirally-coiled twisted-ducts using nanofluid", *Appl. Therm. Eng.*, **143**, 358 (2018).

[12] Ngo, T. L., Kato, Y., Nikitin, K. and Ishizuka, T., "Heat transfer and pressure drop correlations of microchannel heat exchangers with S-shaped and zigzag fins for carbon dioxide cycles", *Exp. Therm. Fluid Sci.*, **32** (2), 560 (2007).

[13] Zheng, Z., Fletcher, D. F. and Haynes, B. S., "Chaotic advection in steady laminar heat transfer simulations: Periodic zigzag channels with square cross-sections", *Int. J. Heat Mass Transf.*, **57** (1), 274 (2013).

[14] Moraveji, M. K. and Beheshti, A. R., "CFD study of the turbulent forced convective heat transfer of non-newtonian nanofluid", *Iran J. Chem. Eng.*, **11** (2), 92 (2014).

[15] Beigzadeh, R., "The CFD provides data for adaptive neuro-fuzzy to model the heat transfer in flat and discontinuous fins", *Iran J. Chem. Eng.*, **16** (2), 57 (2019).

[16] Cui, X., Guo, J., Huai, X., Zhang, H., Cheng, K. and Zhou, J., "Numerical investigations on serpentine channel for supercritical CO_2 recuperator", *Energy*, **172**, 517 (2019).

[17] Rahimi, M., Shabanian, S. R. and Alsairafi, A. A., "Experimental and CFD studies on heat transfer and friction factor characteristics of a tube equipped with modified twisted tape inserts", *Chem. Eng. Process*, **48** (3), 762 (2009).

[18] Taler, D. and Taler, J., "Simple heat transfer correlations for turbulent tube flow", In E3S Web of Conferences, EDP

Sciences, Vol. 13, 02008 (2017).

[19] Ahsan, M., "Numerical analysis of friction factor for a fully developed turbulent flow using k–ε turbulence model with enhanced wall treatment", *Beni Suef Univ. J. Basic Appl. Sci.*, **3** (4), 269 (2014).

[20] Dutta, P., Saha, S. K., Nandi, N. and Pal, N., "Numerical study on flow separation in 90 pipe bend under high Reynolds number by k-ε modelling", *Eng. Sci. Technol. Int. J.*, **19** (2), 904 (2016).

[21] Rahimi, M., Beigzadeh, R., Parvizi, M. and Eiamsa-ard, S., "GMDH-type neural network modeling and genetic algorithm-based multi-objective optimization of thermal and friction characteristics in heat exchanger tubes with wire-rod bundles", *Heat Mass Transf.*, **52** (8), 1585 (2016).